ELectronics EXpress

LETTER

IEICE Electronics Express, Vol.16, No.3, 1–6

Design of broadband power amplifier based on series of continuous inverse modes with phase shift

Gang Liu[1,2], Yongqing Leng[1a)], Xin Qiu[1], Fuqi Mu[1], Yang Li[1], and Xuan Peng[1]

[1] *Institute of Microelectronics, Chinese Academy of Sciences, Beijing, 100029, China*

[2] *University of Chinese Academy of Sciences, Beijing, 100049, China*

a) *lengyongqing@ime.ac.cn*

Abstract: In this paper, a phase shift parameter is introduced to the current waveform of the series of continuous inverse modes (SCIMs) to generate complex fundamental and harmonic admittances. The extended design space based on this novel theory can offer alternative solutions for realizing broadband high-efficiency PAs. To verify the method mentioned above, a 0.9–2.1 GHz PA is designed and fabricated. Experimental results show the PA is able to achieve 63.3%–72.1% drain efficiency and 39.9–41.2 dBm saturated output power in the target band.

Keywords: broadband, high efficiency, series of continuous inverse modes, phase shift, power amplifier

Classification: Microwave and millimeter-wave devices, circuits, and modules

References

[1] S. C. Cripps, *et al.*: "On the continuity of high efficiency modes in linear RF power amplifiers," IEEE Microw. Wireless Compon. Lett. **19** (2009) 665 (DOI: 10.1109/LMWC.2009.2029754).

[2] N. Tuffy, *et al.*: "A simplified broadband design methodology for linearized high-efficiency continuous class-F power amplifiers," IEEE Trans. Microw. Theory Techn. **60** (2012) 1952 (DOI: 10.1109/TMTT.2012.2187534).

[3] V. Carrubba, *et al.*: "Exploring the design space for broadband PAs using the novel continuous inverse class-F mode," Microwave Conference IEEE (2011) 333 (DOI: 10.23919/EuMC.2011.6101840).

[4] J. Chen, *et al.*: "Design of broadband high-efficiency power amplifiers based on a series of continuous modes," IEEE Microw. Wireless Compon. Lett. **24** (2014) 631 (DOI: 10.1109/LMWC.2014.2331457).

[5] W. Shi, *et al.*: "A series of inverse continuous modes for designing broadband power amplifier," IEEE Microw. Wireless Compon. Lett. **26** (2016) 525 (DOI: 10.1109/LMWC.2016.2574820).

[6] V. Carrubba, *et al.*: "The continuous inverse class-F mode with resistive second-harmonic impedance," IEEE Trans. Microw. Theory Techn. **60** (2012) 1928 (DOI: 10.1109/TMTT.2012.2189228).

DOI: 10.1587/elex.16.20181094
Received December 13, 2018
Accepted December 27, 2018
Publicized January 23, 2019
Copyedited February 10, 2019

[7] W. Luo, *et al.*: "Design of broadband power amplifier based on a series of novel continuous inverse modes," Electron. Lett. **53** (2017) 685 (DOI: 10.1049/el.2017.0674).
[8] M. Zhang, *et al.*: "Design of broadband inverse class-F based on resistive-reactive series of inverse continuous modes," IEICE Electron. Express **14** (2017) 20170537 (DOI: 10.1587/elex.14.20170537).
[9] J. Xia, *et al.*: "A linearized 2–3.5 GHz highly efficient harmonic-tuned power amplifier exploiting stepped-impedance filtering matching network," IEEE Microw. Wireless Compon. Lett. **24** (2014) 602 (DOI: 10.1109/LMWC.2014.2324752).
[10] P. J. Tasker and J. Benedikt: "Waveform inspired models and the harmonic balance emulator," IEEE Microw. Mag. **12** (2011) 38 (DOI: 10.1109/MMM.2010.940101).

1 Introduction

Broadband high-efficiency PAs are still fascinate many PA researchers due to the rapid development of wireless communication. The Class-J PA [1], seen as the beginning of investigations on continuous modes, offers multiple solutions to achieve high-efficiency operation. Based on the Class-J mode, the concept of continuous modes has been applied to Class-F [2] and inverse Class-F [3]. These continuous modes provide practical theories for designing broadband high-efficiency PAs. Furthermore, a series of continuous modes between Class-J and continuous Class-F has been proposed [4], which can offer more impedance design space. Then, a series of continuous inverse modes are appeared in succession [5, 6].

It is noteworthy that those continuous modes mentioned above require purely reactive harmonic terminations, which make it impractical to design broadband matching network. Therefore, the bandwidth of continuous modes has somewhat discount. Fortunately, this restriction is alleviated by introducing resistive second harmonic loads to the continuous modes, which results in the bandwidth of PAs can exceed an octave at the expense of efficiency and output power.

In this paper, a phase-shifted current waveform is proposed to explore the design space of the SCIMs. The new current waveform contains resistive second harmonic components, and the corresponding impedance design space is different from the previous works [7, 8]. So the proposed method offers an alternative solution for broadband applications.

2 The series of continuous inverse modes with phase shift

The drain voltage of traditional SCIMs PA is shown as follow:

$$V_{DS}(\theta) = V_{DC} \cdot (1 + \alpha \cos\theta + \beta \cos 2\theta) \tag{1}$$

where V_{DC} is the operating voltage, and different values of α and β represent different continuous inverse mode. And the relationship between α and β is expounded in [5].

Considering the resistive second harmonic component introduced by the common method [7], the second harmonic term can be simplified to cosine term

DOI: 10.1587/elex.16.20181094
Received December 13, 2018
Accepted December 27, 2018
Publicized January 23, 2019
Copyedited February 10, 2019

with phase shift. In this context, the current waveform of SCIMs can be modified by introducing a phase shift parameter ϕ.

$$I_{DS}(\theta) = I_{MAX} \cdot (i_{dc} - i_1 \cos(\theta + \phi) + i_3 \cos(3\theta + 3\phi)) \times (1 - \gamma \sin(\theta + \phi)) \tag{2}$$

Where I_{MAX} is the saturated drain current, $i_{dc} = 0.37$, $i_1 = 0.43$, $i_3 = 0.06$, and $-1 \le \gamma \le 1$ [5]. It can be found that the highest harmonic of the current expansion is the fourth harmonic instead of the fifth harmonic in [7, 8], which is less complexity and more accurate for actual PA. In addition, the current waveforms remain unchanged as the parameter ϕ varies.

From (1) and (2), the fundamental and harmonic admittances can be calculated as follow:

$$Y_{1f} = \frac{2}{\alpha} \cdot [(i_1 \cos\phi + i_{dc}\gamma \sin\phi) - j \cdot (i_{dc}\gamma \cos\phi - i_1 \sin\phi)] \cdot G_{opt} \tag{3a}$$

$$Y_{2f} = -\frac{1}{\beta} \cdot (i_1 + i_3)\gamma \cdot (\sin 2\phi - j \cdot \cos 2\phi) \cdot G_{opt} \tag{3b}$$

$$Y_{3f} = \infty \tag{3c}$$

Where $G_{opt} = (1/2) \cdot (I_{MAX}/V_{DC})$ is the optimal fundamental admittance of standard Class-B mode. In this case, $G_{opt} = 1/32\,\mathrm{S}$ is chosen based on the relative parameters provided by the manufacturer. In order to keep the real part of admittances above zero, the parameter ϕ should meet the strict conditions shown as follow:

$$\begin{cases} 0 \le \phi < \arctan\left(-\dfrac{i_1}{i_{dc} \cdot \gamma}\right), & -1 \le \gamma \le 0 \\ -\arctan\left(\dfrac{i_1}{i_{dc} \cdot \gamma}\right) < \phi \le 0, & 0 \le \gamma \le 1 \end{cases} \tag{4}$$

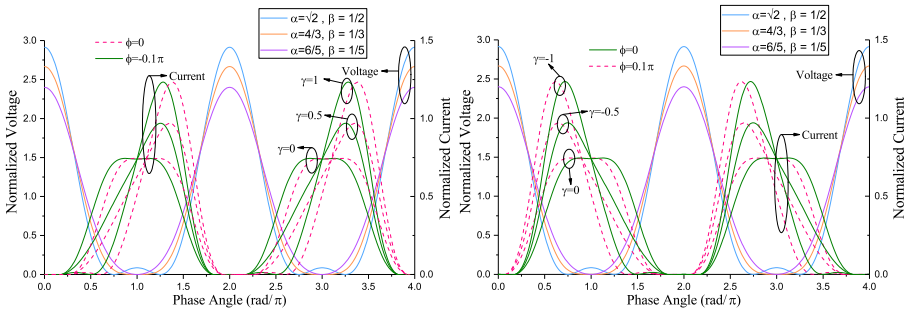

Fig. 1. Normalized current and voltage waveforms with different value of ϕ.

The normalized current and voltage waveforms of SCIMs are presented to show the effect of ϕ, which are shown in Fig. 1. When $\gamma \in [0, 1]$, the current waveforms shift to the right as ϕ exists. In contrast, there is a left shift when $\gamma \in [-1, 0]$.

The fundamental output power P_{out} and drain efficiency η_D are as follow:

DOI: 10.1587/elex.16.20181094
Received December 13, 2018
Accepted December 27, 2018
Publicized January 23, 2019
Copyedited February 10, 2019

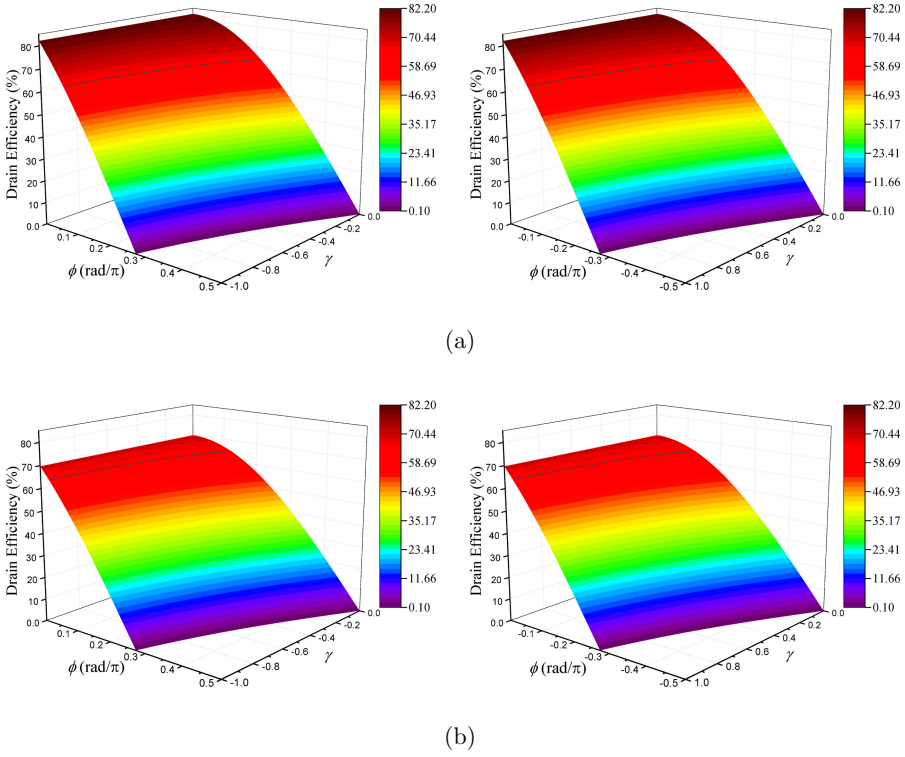

(a)

(b)

Fig. 2. Theoretical drain efficiency versus ϕ and γ. (a) $\alpha = \sqrt{2}$. (b) $\alpha = 6/5$.

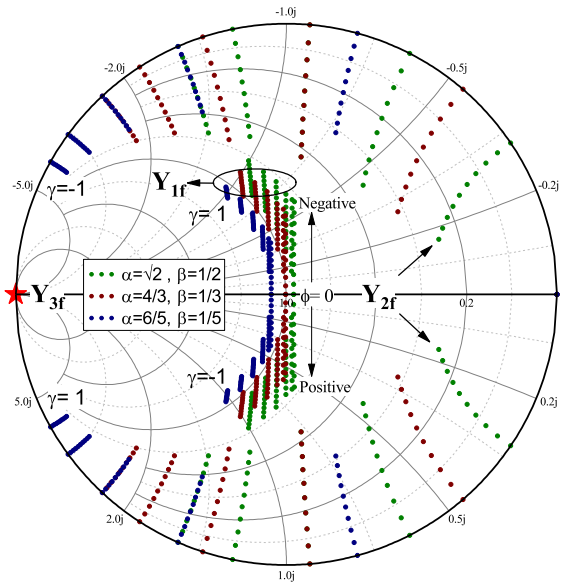

Fig. 3. Admittance design space for $\eta_D > 65\%$, when $\alpha = \sqrt{2}$, $\alpha = 4/3$, $\alpha = 6/5$.

$$P_{out} = \frac{V_{DC} \cdot I_{MAX}}{2} \cdot \alpha(i_1 \cos\phi + i_{dc}\gamma \sin\phi) \tag{5}$$

$$\eta_D = \frac{\alpha}{2 \cdot i_{dc}} \cdot (i_1 \cos\phi + i_{dc}\gamma \sin\phi) \tag{6}$$

Note that the formulas mentioned above depend on α, γ and ϕ. When $\alpha = \sqrt{2}$ and $\alpha = 6/5$, the corresponding η_D with respect to γ and ϕ are plotted in Fig. 2.

DOI: 10.1587/elex.16.20181094
Received December 13, 2018
Accepted December 27, 2018
Publicized January 23, 2019
Copyedited February 10, 2019

Obviously, selecting a proper ϕ can guarantee the drain efficiency exceeding 65% when γ ranges from -1 to 1.

By combining (3) and (5), the admittance design space for the η_D over 65% is obtained, as shown in Fig. 3. The loads at $\alpha = \sqrt{2}$, $\alpha = 4/3$, and $\alpha = 6/5$ are plotted to show the expansion on the design space. It can be seen that the second harmonic admittance is no longer pure reactance, and the corresponding design space is extended in an alternative manner compared to [7] and [8].

3 PA implementation and measurements

Based on the design space proposed above, a wideband PA operating over 0.9–2.1 GHz is designed using GaN HEMT CGH40010F. The drain voltage is set at 28 V with a quiescent current of 68 mA. The circuit is implemented on Rogers 4350B substrate with a thickness of 30 mil.

Constructing the stepped-impedance filter matching network [9] is the most effective method for realizing impedance matching. In this design, a stepped-impedance microstrip-line bandpass network is employed.

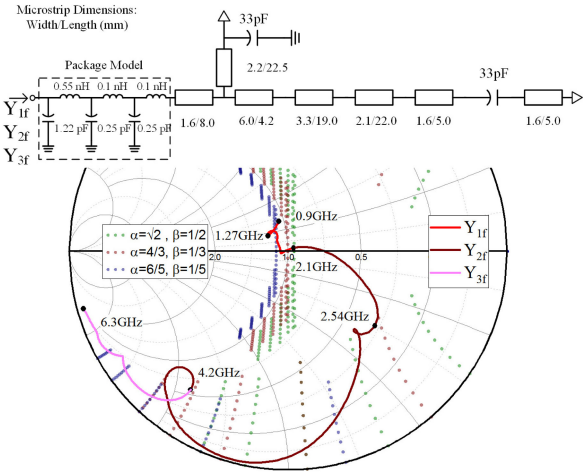

Fig. 4. The synthesized output matching network and the corresponding simulation curves at I-gen plane on Smith chart.

Using the package parasitic model presented in [10], the output impedance can be derived at current-generator plane. Fig. 4 shows the synthesized output matching network and the corresponding impedance trajectory at I-gen plane.

Considering the effect of parasitic parameters and the bandwidth over an octave, the fundamental impedance mathcing is the most important. It can be seen that the fundamental admittances are in conformity with the analysis. However, the second harmonic terminations do not meet the analysis from 0.9 to 1.27 GHz due to the bandwidth over an octave, which will cause the degradation of drain efficiency. In contrast, the results of the second harmonic matching are acceptable in the range of 1.27–2.1 GHz. Therefore, the PA works at the whole novel SCIMs. Although Y_{3f} does not completely fall in the theoretical matching space, the results basically meet the design requirements.

The simulated and measured results with continuous wave signal across the whole operation band are shown in Fig. 5. It can be seen that the measured darin

DOI: 10.1587/elex.16.20181094
Received December 13, 2018
Accepted December 27, 2018
Publicized January 23, 2019
Copyedited February 10, 2019

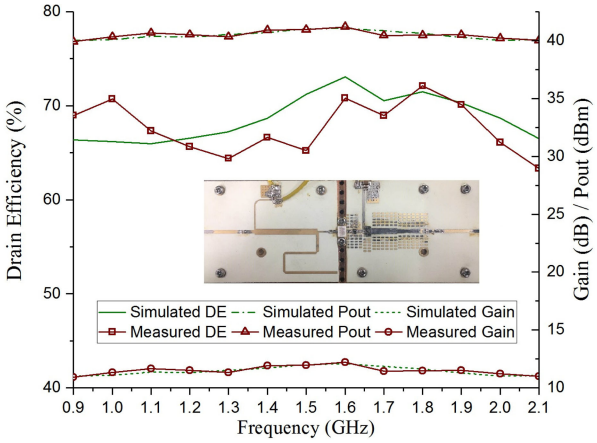

Fig. 5. Simulated and measured results of this design with photograph of the fabricated PA.

Table I. Comparison of some published PAs and our work

Ref	Bandwidth (GHz), (%)	Power (dBm)	η_D (%)	Gain (dB)
[2]	1.45–2.45, 51	40.4–42.2	70–81	10–12.6
[7]	1.8–3.0, 50	41.1–43.2	65–78	10–13.3
[8]	2.5–4.1, 48	39.6–42.6	47–75	8–14
[9]	2.0–3.5, 55	40.5–42	64–76	10.5–12
This work	0.9–2.1, 80	39.9–41.2	63.3–72.1	10.9–12.1

efficiency of 63.3%–72.1%, the output power of 39.9–41.2 dBm, the gain greater than 10.9 dB are achieved. Compared with the simulated results, the measured results of output power and gain are basically the same. Although there are some deviations in the measured drain efficiency, the overall results are acceptable. Table I gives the comparison of our work with others.

4 Conclusion

A series of continuous inverse modes with phase shift is presented in this paper. Based on the new expression of the current waveform, the admittance design space is derived mathmatically. Using the optimal admittances, a broadband PA with high efficiency is implemented based on this theory. A good performance has been verified across the band of 0.9 to 2.1 GHz.

Acknowledgments

This work was supported by the National Natural Science Foundation of China under Grant 61501455 and Natural Science Foundation of Beijing Municipality under Grant 4162068.

DOI: 10.1587/elex.16.20181094
Received December 13, 2018
Accepted December 27, 2018
Publicized January 23, 2019
Copyedited February 10, 2019